The Hippo pathway terminal effector TAZ/WWTR1 mediates oxaliplatin sensitivity in HCT116 colon cancer cells

Věra Slaninová [1#], Lisa Heron-Milhavet[1#], Mathilde Robin[1,2,3], Laura Jeanson[1], Diala Kantar[1], Diego Tosi[1,3], Laurent Bréhélin[2], Céline Gongora[1*], and Alexandre Djiane[1*]

[1] IRCM, Univ Montpellier, Inserm, ICM, Montpellier, France

[2] LIRMM, Univ Montpellier, Inserm, CNRS, Montpellier, France

[3] Fondazione Gianni Bonadonna, Milan, Italy

*Authors for correspondence: IRCM, Inserm U1194
208, rue des Apothicaires
34298 Montpellier, Cedex, France
tel: +33 (0) 411 283 157
email: alexandre.djiane@inserm.fr
celine.gongora@inserm.fr

# contributed equally

KEY WORDS:

Oxaliplatin, colon cancer, Hippo signaling, TAZ, P53

SUMMARY

YAP and TAZ, the Hippo pathway terminal transcriptional activators, are frequently upregulated in cancers. In tumor cells, they have been mainly associated with increased tumorigenesis controlling different aspects from cell cycle regulation, stemness, or resistance to chemotherapies. In fewer cases, they have also been shown to oppose cancer progression, including by promoting cell death through the action of the P73/YAP transcriptional complex, in particular after chemotherapeutic drug exposure. We show here that oxaliplatin treatment on colorectal cancer HCT116 cells led to a dramatic core Hippo pathway down-regulation and nuclear accumulation of TAZ. We further show that TAZ was required for the increased sensitivity of HCT116 cells to oxaliplatin, an effect that appeared independent of P73, but which required the nuclear relocalization of TAZ. Our results support thus an early action of TAZ to sensitize cells to oxaliplatin, consistent with a model in which nuclear TAZ in the context of DNA damage and P53 activity pushes cells towards apoptosis.

INTRODUCTION

Colorectal cancer (CRC) is the third leading cause of cancer-related death worldwide (Rawla et al., 2019). 30% of patients present synchronous metastases and 50-60% will develop metastases that will require chemotherapy. The current management of advanced or metastatic CRC is based on fluoropyrimidine (5-FU), oxaliplatin and irinotecan as single agents or more often in combination (e.g. FOLFOX, FOLFIRI, or FOLFIRINOX; Xie et al., 2020). Chemotherapy is combined with targeted therapy including monoclonal antibodies against EGFR (e.g. cetuximab and panitumumab) or VEGF (bevacizumab), tyrosine kinase inhibitors (e.g. regorafenib), and immune checkpoint blockade agents for patients with MSI-High tumors (e.g. pembrolizumab; Xie et al., 2020).

Oxaliplatin is a third-generation platinum antitumor compound with a 1,2-diaminocyclohexane (DACH) ligand (Chaney, 1995; Raymond et al., 1998). It induces mainly intra-strand crosslinks, but also inter-strand crosslinks and DNA-protein crosslinks that stop DNA replication and transcription, leading to apoptotic cell death (Perego and Robert, 2016; Woynarowski et al., 2000, 1998). Oxaliplatin exerts its anti-tumor effect also by inducing immunogenic cell death (Tesniere et al., 2010). Resistance to oxaliplatin can be either intrinsic (primary resistance) or acquired (secondary resistance), and is usually tackled by combining drugs to expose tumoral cells weaknesses or inhibit alternative survival pathways (Vasan et al., 2019). Despite intense research efforts in this field, more information on the molecular mechanisms underlying oxaliplatin mechanism of action are needed to develop new treatment strategies and improve the therapeutic response rate.

The Hippo signaling pathway represents an evolutionarily highly conserved growth control pathway. First discovered through genetic screens in *Drosophila*, it consists of a central cascade of core kinases: MST1/2 and LATS1/2 (homologues of *Drosophila* Hippo and Warts; Heng et al., 2021; Pocaterra et al., 2020; Zheng and Pan, 2019). When activated, LATS1/2 phosphorylate YAP and WWTR1/TAZ (homologues of *Drosophila* Yki), two partly redundant transcriptional co-activators which represent the terminal effector of the Hippo pathway (Reggiani et al., 2021). Phosphorylated YAP and TAZ are retained in the cytoplasm through binding to 14-3-3 proteins, and sent for proteasomal degradation. When the Hippo pathway is not activated, hypo-phosphorylated YAP/TAZ enter the nucleus and bind to specific transcription factors (TFs) to turn on the transcription of target genes. The best characterized TF partners for YAP and TAZ are the TEADs (TEAD1-4, homologues of *Drosophila* Scalloped; Heng et al., 2021; Pocaterra et al., 2020; Zheng and Pan, 2019). While depending

73 on cell type, the classic target genes include genes involved in proliferation, resistance to
74 apoptosis, cytoskeletal remodeling, or stemness (Rosenbluh et al., 2012; Tapon et al., 2002;
75 Totaro et al., 2018). But YAP/TAZ nucleo-cytoplasmic localization (and activity) is also
76 controlled by mechanical cues relayed by the actin cytoskeleton, or by cytoplasmic trapping
77 proteins such as AMOTs (Heng et al., 2021; Pocaterra et al., 2020; Zheng and Pan, 2019).
78 Importantly, the nuclear retention of YAP and TAZ is favored by tyrosine phosphorylation by
79 different kinases, and in particular SRC and YES (Byun et al., 2017; Ege et al., 2018; Li et al.,
80 2016).

81 The Hippo pathway has been primarily described as a tumor suppressive pathway in a wide
82 variety of solid tumors (Kim and Kim, 2017; Li and Guan, 2022; Nguyen and Yi, 2019;
83 Thompson, 2020; Zheng and Pan, 2019) preventing the pro-tumoral effect of YAP/TAZ.
84 However, in CRCs the role of the Hippo pathway and of YAP and TAZ appears more complex.
85 Several studies point towards a classic pro-tumoral role for YAP and TAZ. In CRC patients
86 tumor samples, high expression and nuclear localizations of YAP correlated strongly with
87 disease evolution and bad prognosis (Ling et al., 2017; Steinhardt et al., 2008), or with
88 resistance to treatments such as 5FU or cetuximab (Kim and Kim, 2017; Lee et al., 2015; Touil
89 et al., 2014). Furthermore, invalidating YAP could blunt tumorigenic behaviors both in mice
90 CRC models (Shao et al., 2014) or in the metastatic HCT116 CRC cell line (Konsavage et al.,
91 2012). However, YAP could exhibit a tumor suppressive role in CRCs. Studies in genetic
92 mouse models have shown that YAP/TAZ restricts canonical Wnt/β-Catenin signaling thus
93 preventing intestinal stem cells amplification, and could act as tumor suppressors in CRCs
94 (Azzolin et al., 2014, 2012; Barry et al., 2013). Similarly, the loss of core Hippo kinases
95 (LATS/MST) was recently shown to inhibit tumor progression in Apc mutant mouse models
96 and in patients-derived xenografts models (Cheung et al., 2020; Li et al., 2020).

97 The tumor suppressive role of YAP in CRC is further supported by its reported role in response
98 to DNA damage inducer drugs. Studies have shown that, in different cell lines including CRC
99 lines, cell death in response to cisplatin, doxorubicin, or etoposide, is mediated by P73, a
100 protein related to the tumor-suppressor P53. Following treatments, a YAP/P73 complex
101 accumulates in the nucleus, and triggers the transcription of P73 target genes involved in cell
102 death (Lapi et al., 2008; Strano et al., 2005, 2001). The direct interaction between YAP and
103 P73 is proposed to prevent P73 destabilization by the E3-Ubiquitin Ligase ITCH (Levy et al.,
104 2007; Strano et al., 2005). This pro-apoptotic role of YAP is reminiscent to a similar role of
105 Yki in *Drosophila* (a Yki/p53 complex; (Di Cara et al., 2015). Importantly, this appears specific

106 to YAP, since TAZ cannot bind to P73, further suggesting that YAP and TAZ, while
107 performing redundant roles, also possess specific activities (Reggiani et al., 2021).

108 Given that oxaliplatin constitute one of the most used drugs in the treatment of CRCs, it is
109 important to evaluate its effects with respect to the Hippo pathway and to YAP/TAZ which can
110 elicit conflicting roles to oppose or promote CRC tumorigenesis. We show here that upon
111 treatment with oxaliplatin, the core Hippo pathway was inhibited in HCT116 cells leading to
112 TAZ accumulation and nuclear re-localization. We further show that TAZ was required for
113 early sensitivity of HCT116 to oxaliplatin. Interestingly, the nuclear localisation of TAZ was
114 important, and drugs preventing this such as Dasatinib antagonized the effect of oxaliplatin.
115 These results support an early anti-tumoral role of YAP and TAZ in response to oxaliplatin
116 suggesting particular attention to sequence of treatments and drug combinations should be paid
117 when considering potential future drugging of YAP/TAZ signaling in the treatment of CRCs.

118

119 **RESULTS and DISCUSSION**

120 ***Oxaliplatin treatment triggers an early cell death program***

121 Oxaliplatin is a third generation platinum compound widely used as part of the first line of
122 treatment for colon cancer patients in the FOLFOX regimen (Chaney, 1995; Raymond et al.,
123 1998; Xie et al., 2020). Inside cells, oxaliplatin binds DNA, generating adducts which
124 ultimately lead to DNA breaks and replicative stress in proliferating cells. When used on
125 proliferating cancer cells, oxaliplatin treatment resulted in concentration-dependent cell death.
126 We measured the IC50 of oxaliplatin on HCT116 colon cancer cells at 0.5µM (Supplemental
127 Figure 1A). This dose reduced the amount of cells by 50% after 4 days of treatment. This dose
128 was about 10 fold lower than the oxaliplatin concentration reported in the blood of treated
129 patients (between 3.7 and 7µM; Graham et al., 2000). The oxaliplatin dose used in this study
130 was thus compatible with the dose that could be ultimately found at the level of tumors in a
131 clinical setting, and did not represent an acute high concentration treatment, highlighting its
132 relevance for studying cellular responses to oxaliplatin.

133 When treated with oxaliplatin at IC50, HCT116 cells exhibited clear signs of DNA damage
134 such as accumulation of γH2AX, and 53BP1 puncta in the nuclei (Figure 1A&B). Consistently,
135 P53, which has been shown to control a specific cell death program in response to severe DNA
136 damage (for recent reviews, (Abuetabh et al., 2022; Panatta et al., 2021), accumulated strongly
137 24h after treatment (Figure 1C). Intriguingly, the P53 related protein P73, previously reported
138 to accumulate and to mediate cell death in response to DNA-damage inducing drugs such as
139 cisplatin, doxorubicin or etoposide, including in HCT116 cells (Lapi et al., 2008; Strano et al.,
140 2005), was destabilized upon oxaliplatin treatment. P63, the third member of the P53 protein
141 family, was not expressed in HCT116, even upon treatment (Figure 1C).

142 To better understand the cellular responses to oxaliplatin we profiled the changes in gene
143 expression after 24h of exposure at IC 50. This analysis revealed that the expression of only a
144 limited number of genes were affected (fold change >1.5, adjusted p-value < 0.05): 253 up-
145 regulated and 111 down-regulated (Figure 1D; Supplemental Table 1). Gene ontology
146 enrichment approaches using the g:profiler online tool (Supplemental Table 2; Raudvere et al.,
147 2019) highlighted that amongst the main cellular processes controlled by the upregulated genes
148 were DNA damage response (GO:0044819 mitotic G1/S transition checkpoint signaling;
149 GO:0000077 DNA damage checkpoint signaling…), apoptosis and cell death (GO:0045569
150 TRAIL binding; GO:0008219 cell death; GO:0012501 programmed cell death; GO:0006915
151 apoptotic process …), and p53 response (GO:0072331 signal transduction by p53 class

152 mediator), consistent with the known role of oxaliplatin generating adducts on the DNA.
153 Indeed, many genes up-regulated have previously been associated with p53 signaling, and
154 represent p53 canonical target genes such as CDKN1A/P21, P53I3, BAX, or TIGAR
155 (REAC:R-HSA-3700989 Transcriptional Regulation by P53; WP:WP4963 p53 transcriptional
156 gene network). While up-regulated genes controlled mainly cell death programs, the down-
157 regulated genes were involved in DNA replication (GO:0006260) and cell cycle (GO:0007049)
158 consistent with the well documented effect of DNA damage on blocking cell cycle and
159 proliferation (Abuetabh et al., 2022).
160 Amongst the genes mis-regulated were also genes related to inflammation and immune cell
161 recruitment (e.g. the upregulated genes CXCR2, EBI3/IL-27, or NLRP1, and the
162 downregulated gene IL17RB) consistent with the previously reported role of oxaliplatin during
163 immune cell death (Tesniere et al., 2010).
164 Finally, these analyses also highlighted several genes involved in cell architecture, namely
165 cytoskeleton and junctional complexes. Amongst the most striking features were changes in
166 the expression of integrin and extracellular matrix proteins engaging Integrins and Focal
167 Adhesions: collagens COL5A1 and COL12A1, as well as laminins LAMA3, LAMB3, and
168 LAMC1 and integrin ITGA3. These observations suggest that treated cells might remodel their
169 extracellular matrix, their Focal Adhesions, and the signaling pathways associated. The RNA-
170 Seq analyses revealed also many changes to the cytoskeleton, including an upregulation of
171 several keratin-based intermediate filaments (KRT15/19/32) and associated factors (KRTAP2-
172 3 and SFN). Several genes controlling the actin cytoskeleton were also affected such as the
173 branched actin regulators WDR63, CYFIP2, or WASF3, or different genes predicted to control
174 RHO activity (up: RHOD, EZR, and RAP2; down: ARHGAP18).
175
176 Taken together, these results suggest that upon oxaliplatin treatment, HCT116 cells implement
177 an early cell death program, which is likely mediated by the elevated P53 levels, and many
178 "bona-fide" P53 direct target genes involved in cell death are upregulated. Unlike other
179 treatments such as cisplatin, doxorubicin, and etoposide (Lapi et al., 2008; Strano et al., 2005),
180 oxaliplatin is unlikely to mobilize the p73 anti-tumoral response since P73 levels are decreased
181 upon oxaliplatin treatment. The difference is striking when considering closely related
182 platinum compounds such as cisplatin and oxaliplatin. This difference is unlikely due to timing
183 as we could not observe any P73 up-regulation after oxaliplatin treatment even after shorter or
184 longer exposures. Even though dose comparisons between different compounds is tricky, we
185 note that the cisplatin dose was 50 times higher than that of oxaliplatin. Alternatively, while

186 both are thought to act primarily as generators of lethal amounts of DNA breaks, their
187 difference in mobilizing either P73 (cisplatin) or P53 (oxaliplatin) might arise from different
188 alternative cellular effects independent of DNA damage.
189
190 ***Oxaliplatin treatment triggers YAP and TAZ nuclear accumulation***
191 Having established a regimen for treating HCT116 cells with oxaliplatin, and given the
192 complex reported roles of YAP/TAZ in CRCs (see Introduction), we investigated whether
193 YAP/TAZ could be affected, and thus monitored TEAD, YAP, and TAZ expressions and
194 localizations following oxaliplatin treatment.
195 After 24h (or 48h) of oxaliplatin treatment at the IC50, we did not observe any change in the
196 total levels or in the nuclear localization of TEAD4, the main TEAD paralogue in colon cells
197 (Figure 2A). However, TAZ and YAP nuclear localizations increased following oxaliplatin
198 treatment in our culture conditions: the TAZ and YAP nuclear staining increased by 60% and
199 55% respectively when compared to untreated cells (Figure 2A). TAZ nuclear accumulation
200 was further confirmed by fractionation experiments (Figure 2C; see Materials and Methods).
201 This increase in TAZ nuclear localization was reflected by an increase in total TAZ levels by
202 western blot analysis (Figure 2B). However, YAP total levels, and more importantly the levels
203 of YAP phosphorylation on Serine 127 (S127) were unchanged (Figure 2B).
204 The YAP S127 phosphorylation is deposited by the LATS1/2 Hippo pathway terminal kinases
205 and mediate the cytoplasmic retention of YAP by the 14-3-3 proteins and later targeting for
206 proteasomal degradation (Heng et al., 2021; Pocaterra et al., 2020; Zheng and Pan, 2019).
207 Western-blot analyses on total protein extracts showed that several key proteins in the core
208 Hippo pathway were hypo-phosphorylated (p-MST1/2, p-MOB1) indicating a general lower
209 activity of the core Hippo pathway (Figure 2B). Total protein levels were also lower after
210 treatment, further suggesting a lower Hippo pathway activity in response to oxaliplatin,
211 consistent with the increased TAZ levels and increased nuclear TAZ localization (Figure
212 2A&C). However, given that levels of phospho-YAP and total YAP remained unchanged, how
213 the Hippo pathway down-regulation could have differing effects on YAP and TAZ remains to
214 be explored. YAP and TAZ appear only partly redundant, and YAP and TAZ specific
215 regulations have been reported (Reggiani et al., 2021). It is noteworthy that an additional
216 phospho-degron is present in TAZ, making it more sensitive to degradation than YAP. This
217 increased sensitivity might magnify TAZ level changes when the Hippo pathway is inhibited
218 by oxaliplatin (Azzolin et al., 2012). The decreased protein levels of different Hippo pathway
219 components in response to oxaliplatin were unlikely due to reduced mRNA abundance, since

220 we did not observe any change in our RNA-Seq, suggesting that it might be a consequence of
221 reduced translation and/or increased protein degradation. Indeed, previous studies have shown
222 that core Hippo pathway components can be regulated by ubiquitination such as LATS1 or
223 MOB1 (Ho et al., 2011; Lignitto et al., 2013; Salah et al., 2011). Whether oxaliplatin treatment
224 triggers a specific ubiquitin-mediated destabilization of the core Hippo pathway remains
225 however to be studied.
226
227 ***YAP is dispensable for Oxaliplatin-mediated cell death***
228 Performing pathway analyses on the mis-regulated genes highlighted a strong activation of p53
229 signaling (Supplemental Table S2). Motif enrichment analyses suggested that the p53 family
230 of transcription factors were the main controllers of the up-regulated genes. With the exception
231 of Axl, none of the "classic" YAP/TAZ target genes such as CTGF, CYR61/CCN1, or BIRC2
232 (or genes involved in cell cycle progression, cytoskeleton regulation, or drug resistance;
233 (Pocaterra et al., 2020; Totaro et al., 2018) were up-regulated after oxaliplatin treatment. We
234 thus wondered what would be the role of YAP and TAZ in the response to oxaliplatin treatment.
235 Indeed, other anti-cancer drugs such as cisplatin have been shown to promote cell death in part
236 through the implementation of a P73/YAP-dependent cell death program. Mechanistically, it
237 has been proposed that DNA damage induced by cisplatin stabilizes YAP which then binds
238 and protects P73 from ITCH-mediated degradation (Levy et al., 2007); the P73/YAP complex
239 accumulates in the nucleus to turn on the expression of P73 target genes involved in cell death
240 (Lapi et al., 2008; Strano et al., 2005, 2001). We thus wondered whether the accumulation of
241 TAZ (and the moderate accumulation of YAP) in the nucleus could also participate in the cell
242 death induced by oxaliplatin.
243 To test the requirement of YAP and TAZ, we invalidated YAP and TAZ by RNA interference.
244 The sole invalidation of YAP by shRNA led to a very modest reduction in oxaliplatin
245 sensitivity (IC50 in *shYAP* was determined at 0.62 compared to 0.52 in *shLuc* controls) (Figure
246 3A&C). It is noteworthy that, under the culture conditions used, YAP appeared dispensable for
247 HCT116 cells since the shRNA led to a knock-down efficiency >90%. These results suggest
248 that the cell death in response to oxaliplatin might not be dependent (or only marginally) on
249 the YAP/P73 complex as previously reported for other DNA-damage inducing compounds
250 (Lapi et al., 2008; Levy et al., 2007; Strano et al., 2005), but depends on alternative
251 mechanisms.
252
253 ***TAZ promotes cell death in response to oxaliplatin, independently of P73***

254 We then investigated the role of TAZ. Strikingly, while the depletion of YAP had hardly any
255 effect, the combined knock-down of both YAP (shYAP) and TAZ (siTAZ), resulted in a clear
256 increase in resistance to oxaliplatin, where the IC50 reached 0.91µM in *shYAP/siTAZ* HCT116
257 cells compared to 0.58µM in *shLuc/siScrambled* HCT116 control cells (Figure 3B&C),
258 highlighting that TAZ participates to cell death in response to oxaliplatin. We then wondered
259 whether the increased sensitivity promoted by TAZ could be dependent on P73, in a similar
260 mechanism as proposed for cisplatin. However, while P53 accumulated in response to
261 oxaliplatin in HCT116, P73 levels were decreased, undermining the role of P73 in response to
262 this drug (Figure 1C). This absence of P73 stabilization, is consistent with the absence of
263 increased YAP levels after oxaliplatin treatment (Figure 2B). These results highlight that,
264 although overexpressed YAP could bind and stabilize endogenous P73 (Supplemental Figure
265 2; (Levy et al., 2007; Strano et al., 2005, 2001), oxaliplatin treatments at the clinically relevant
266 doses used, do not lead to YAP and P73 stabilization. We then confirmed that TAZ cannot bind
267 P73 (Supplemental Figure 2), ruling out that the elevated nuclear TAZ following oxaliplatin
268 could act through a transcriptional complex with P73 to enhance cell death. A recent study
269 reported a direct interaction between TAZ and P53 in MCF7 and HCT116 cells, which resulted
270 in the inhibition of P53 activity towards senescence (Miyajima et al., 2020). However, when
271 we performed co-immunoprecipitation experiments, we were unable to document any
272 interaction between over-expressed YAP or overexpressed TAZ with endogenous P53 in
273 normal or oxaliplatin treated HCT116 cells (Supplemental Figure 2). Furthermore, the
274 increased oxaliplatin resistance of cells upon *YAP/TAZ* knockdown supports strongly that TAZ
275 acts to promote cell death and thus cooperates with P53 rather than antagonizes its activity as
276 suggested before (Miyajima et al., 2020). Taken together, these results suggest that the
277 sensitivity of HCT116 cells to oxaliplatin mediated by YAP and TAZ is not mediated by the
278 direct interaction of YAP or TAZ to P53 or P73.
279
280 ***Increased resistance to oxaliplatin upon YAP/TAZ activity blockade***
281 The sh/siRNA interference results suggested that TAZ was required for sensitivity to
282 oxaliplatin. To validate independently the knock-down experiments, we used a
283 pharmacological approach with drugs targeting YAP/TAZ activity and monitored their action
284 in combination with oxaliplatin. We performed 2D matrices co-treatment analyses in which
285 cells were treated with increasing amounts of oxaliplatin and of the YAP/TAZ inhibitors
286 verteporfin or CA3 (Figure 3D and Supplemental Figure 1B &C; Liu-Chittenden et al., 2012;
287 Song et al., 2018). In both cases, the co-treatments led to a marked increase in the HCT116

288 resistance to oxaliplatin. The mode of action of verteporfin remains unclear and might involve
289 increased retention in the cytoplasm of YAP and TAZ, or their degradation, preventing them
290 from complexing in the nucleus with their transcription factor partners (Wang et al., 2016). A
291 recent study showed that CA3 reduced the transcriptional activity mediated by YAP/TAZ-
292 TEAD (reduction in target genes expression), with only minor effects on YAP protein levels
293 (Morice et al., 2020). Even though the exact mode of action of verteporfin and CA3 remain
294 unclear, the increased resistance to oxaliplatin observed by co-treating cells with YAP/TAZ
295 pharmacological inhibitors, confirms the results obtained with the genetic knock-down, and
296 supports a model where increased TAZ activity participate in the sensitivity of HCT116 cells
297 to oxaliplatin.
298
299 ***Src inhibition by Dasatinib reduces HCT116 cells sensitivity to oxaliplatin***
300 The results suggest thus that preventing TAZ signaling in the early phases of oxaliplatin
301 treatment would represent a counter-productive approach, leading to reduced efficacy of
302 oxaliplatin to induce cell death. Besides the canonical Hippo signaling pathway, the nucleo-
303 cytoplasmic shuttling of YAP and TAZ is under the control of many other inputs. In particular,
304 YAP and TAZ retention in the nucleus is promoted by the action of different tyrosine kinases,
305 such as ABL or SFKs (Src Family Kinases) which phosphorylate the C-termini of YAP and
306 TAZ (Y357 or Y316 respectively; Byun et al., 2017; Ege et al., 2018; Guégan et al., 2022;
307 Kedan et al., 2018; Lamar et al., 2019; Li et al., 2016). Due to its high relevance for colon
308 cancer, we focused our analysis on SRC, frequently activated in colon carcinoma (Sirvent et
309 al., 2020). An earlier study showed that depending on the colon cancer cell line considered,
310 SRC could be activated, inhibited, or not affected following oxaliplatin treatment (Kopetz et
311 al., 2009). We could replicate that SRC was not activated after 24h of oxaliplatin treatment in
312 HCT116 cells (as measured by phosphorylation on Y416; Figure 4A). Working with HCT116,
313 we are thus in a position to test the contribution of SRC to YAP/TAZ shuttling during
314 oxaliplatin treatment without the complications arising from treatment-induced acute SRC
315 activation. Previous reports suggested that the classic SRC kinase inhibitor Dasatinib could be
316 used as a drug to prevent YAP/TAZ signaling (Rosenbluh et al., 2012). Indeed, combining
317 Dasatinib with oxaliplatin treatment, prevented the nuclear accumulation of TAZ (Figure 4B).
318 The addition of Dasatinib to oxaliplatin treated cells led to a dramatic reduction of the TAZ
319 nuclear staining when compared to oxaliplatin alone (95% reduction; see Materials and
320 Methods). It should be noted however, that Dasatinib treatment at 50nM reduced slightly the
321 elevated global TAZ levels observed in response to oxaliplatin (Figure 4A). Nevertheless, even

322 though TAZ appeared a bit more unstable in presence of Dasatinib, its nucleo-cytoplasmic ratio
323 was still profoundly affected by Dasatinib, preventing nuclear accumulation (Figure 4B).
324 We thus asked what would be the combined effect of Dasatinib treatment and oxaliplatin in
325 HCT116 cells. We thus performed 2D matrices co-treatment analyses in which cells were
326 treated with increasing amounts of oxaliplatin and of Dasatinib using drug ranges
327 encompassing their respective IC50 (0.5µM for oxaliplatin and 8µM for Dasatinib;
328 Supplemental Figure 1A&D). Strikingly combining both drugs showed clear regions of
329 antagonism, suggesting that Dasatinib treatment reduced HCT116 cells sensitivity to
330 oxaliplatin (Figure 4C). These results further support a model in which the nuclear
331 relocalization of TAZ in response to oxaliplatin treatment sensitizes cells, and caution the use
332 of Dasatinib in combination to oxaliplatin.
333
334 ***YAP/TAZ promote cell death in the early response to chemotherapeutic agents***
335 Taken together the results presented here show that oxaliplatin promotes the fast nuclear
336 relocalization of TAZ which then participates to the cells sensitivity to oxaliplatin. Given that
337 we could not find any interaction between TAZ and P53 family members, but that the nuclear
338 localization of TAZ is required for its effect, we could envision several models:
339 i) either the TAZ/TEAD transcription complex, in the context of DNA damage and P53
340 activation, promotes the transcription of specific early response genes promoting cell death;
341 ii) or the slight increase at the transcriptional level of "classic" YAP/TAZ/TEAD targets
342 involved in proliferation sensitizes cells to DNA damage and replicative stress;
343 iii) or alternatively, TAZ acts through a new complex involved in cell death, independently of
344 TEAD.
345 More studies should help to distinguish between these potential models.
346
347 YAP and TAZ, have been implicated in the resistance to various chemotherapies or targeted
348 therapies in different cancers (Kim and Kim, 2017; Nguyen and Yi, 2019; Zeng and Dong,
349 2021). It should be noted that the current study focuses on the immediate effects of oxaliplatin
350 within the first hours after exposure. Whether YAP and TAZ are later important for the
351 maintenance of the resistance acquired by the surviving clones is not addressed in this study.
352 Hints towards this later role of YAP/TAZ, are suggested by the elevated YAP levels reported
353 in many cancer cells following resistant clone selection (our own unpublished results, and Kim
354 and Kim, 2017; Nguyen and Yi, 2019; Zeng and Dong, 2021). Functional studies impairing
355 YAP demonstrated that YAP is indeed required for the tumorigenicity of resistant cells

356 (Yoshikawa et al., 2015). Furthermore, elevated YAP and TAZ nuclear staining is frequently
357 observed in patients tumor samples, including in CRCs (Li and Guan, 2022; Ling et al., 2017;
358 Steinhardt et al., 2008; Thompson, 2020). In advanced cancers, almost all patients undergo one
359 or more rounds of treatment before surgery, if surgery is possible. It is thus unclear whether
360 the increased YAP/TAZ nuclear levels observed in tumor samples reflect primary response to
361 treatment (as suggested by the current study), or whether they represent a secondary state that
362 might have been selected in the cells resistant to treatment.
363 The current study investigates the early response to oxaliplatin, supporting an early tumor
364 suppressive role of YAP/TAZ in response to treatment, in which, in the context of detrimental
365 DNA damage, YAP/TAZ activity promotes cell death. Is this role general or is it specific to
366 CRCs and oxaliplatin? Independently of the mechanism involved (YAP/P73 complex as
367 previously reported or alternative TAZ-mediated mechanisms as shown here), different breast
368 and colon cancer cell lines mobilize YAP or TAZ to promote cell death in response to many
369 different DNA damaging agents (Basu et al., 2003; Lapi et al., 2008; Levy et al., 2007; Strano
370 et al., 2005, 2001). This anti-tumoral role appears evolutionarily conserved and in *Drosophila*
371 the YAP/TAZ homologue Yki promotes cell death in response to different stress inducing
372 agents (Di Cara et al., 2015), further suggesting that YAP/TAZ might promote cell death in
373 response to chemotherapeutic agents in other cancers beside CRCs and breast cancers. When
374 considering drugging YAP/TAZ signaling in the treatment of CRCs and other cancers, special
375 attention should thus be given to drug combinations, and importantly the sequence in which
376 they will be used.
377

378 **MATERIALS AND METHODS**

379 ***shRNA construction***

380 shRNA directed against human *YAP*, *TAZ*, or the non-relevant *Luciferase* gene were designed
381 by adding to the selected targeted sequences, overhangs corresponding to BamHI and EcoRI
382 cloning sites at the 5'end of forward and reverse strand, respectively. Resulting oligos were
383 then annealed together and cloned into the pSIREN-RetroQ vector (TaKaRa) according to the
384 manufacturer's protocol between BamHI and EcoRI cloning sites.

385 Targeted sequences:

386 *shRNA-YAP(3619):* CAATCACTGTGTTGTATAT

387 *shRNA-TAZ(1417):* CCCTTTCTAACCTGGCTGT

388 *shRNA-Luciferase:* CGTACGCGGAATACTTCGA

389

390 ***Cell culture and cell transfections***

391 Human HCT116 colorectal cancer cell line (ATCC 2017) was cultured in RPMI1640
392 supplemented with 10% FBS at 37°C in a humidified atmosphere with 5% CO_2. No antibiotics
393 were used to avoid any cross-reaction with the Oxaliplatin treatment.

394 HCT116 cells expressing shRNA against *YAP*, *TAZ* , or *Luciferase* (Luc; control) were
395 obtained by retroviral gene transduction of the corresponding pSIREN vectors. Retroviral
396 particles were produced in HEK293 cells and subsequently used to infect HCT116 cells.
397 Positive clones were selected with 1 µg/mL puromycin and pooled together.

398 HCT116-*shYAP/siTAZ* cells were created by transfecting 100nM of *TAZ siRNA* (Dharmacon
399 siGENOME SMARTpool #M-016083-00-0005) into HCT116-*shYAP* cells using
400 Lipofectamine 2000 (Invitrogen) according to manufacturer's protocol. As a negative control,
401 100nM of *siScrambled* (D-001206-13) was transfected into HCT116-*shLuc* cells.

402

403 ***RNA-Seq***

404 HCT116 cells were plated to reach 60 to 70% of confluence and treated with 0.5 µM
405 Oxaliplatin (IC_{50}) for 24 hours. RNA was extracted using RNeasy plus mini kit (Qiagen),
406 quantified and analyzed for its integrity number (RIN) using a Bioanalyzer (Agilent 2100 at
407 the IRMB: https://irmb-montpellier.fr/single-service/transcriptome-ngs/). RNA (1 µg) with
408 RIN between 8 and 10 were sent for RNA-Sequencing analysis to Fasteris biotechnology
409 company (http://www.fasteris.com). After library preparation, sequencing was performed on
410 the Illumina NovaSeq 6000 platform (S1 2x100 full FC). Mapping on the human genome

411 GRCh38 was performed using the protocol STAR 2.7.5b leading to 80-100 Millions reads per
412 condition. Normalization and pairwise differential expression analyses were performed using
413 the R package DESeq2 (2.13) (Anders and Huber, 2010).
414 RNA-Seq data has been deposited in NCBI's Gene Expression Omnibus under accession
415 number GSE227315.
416
417 ***Western blotting***
418 Proteins issued from transfected untreated and treated HCT116 cells were extracted, analyzed
419 by SDS-PAGE. Dilutions and antibodies' references are listed below.
420 Flag M2 (1/2000; Sigma-Aldrich #F1804)
421 GAPDH (1/3000; Proteintech #60004)
422 Histone H3 (1/1000; Cell Signaling Technology CST #4499)
423 LATS1 (1/1000; CST #3477)
424 MOB1 (1/1000; CST #13730)
425 p-MOB1 (1/1000; CST #8699)
426 MST1 (1/1000; CST #3682)
427 p-MST1/2 (1/1000; CST #49332)
428 NF2 antibody (Proteintech #26686-1-AP)
429 P53 (1/5000; Proteintech #10442-1-AP)
430 P63 (1/250; Santa Cruz #sc25268)
431 P73 (1/1000; CST #14620)
432 p-SRC Y416(1/1000; CST #2105)
433 TAZ (1/1000; CST #4883)
434 TEAD4 (1/250; Santa Cruz #sc101184)
435 Tubulin (1/10000; Sigma-Aldrich #T6074)
436 YAP (1/1000; CST #14074)
437 p-YAP S127 (1/1000; CST #13008)
438
439 ***Immunoprecipitation and co-immunoprecipitation***
440 Protein extracts were prepared in lysis buffer (NaCl 150 mM, Tris pH 7.4 10 mM, EDTA 1
441 mM, Triton X-100 1%, NP-40 0.5%, cOmplete, EDTA-free protease inhibitors (Roche
442 #11873580001) for 30 min on ice before centrifugation. Immunoprecipitations were performed
443 overnight at 4°C on a rocking wheel using mouse EZview Red anti-Flag M2 affinity gel
444 (Sigma-Aldrich #F1804) after transfections of either p2xFlag CMV2 (empty vector), p2xFlag

445 CMV2-YAP2 (YAP1; Addgene #19045) or p2xFlag CMV2-WWTR1 (TAZ). After Flag
446 immunoprecipitation, washes in lysis buffer were performed, followed by protein elution by
447 competition with 3XFLAG peptide (150 ng/µL final concentration) during 1 hour at 4°C. The
448 different immunoprecipitates were then subjected to Western blotting for detection of protein
449 complexes.
450
451 ***Immunofluorescence***
452 Cells seeded on glass coverslips were fixed 10 min in paraformaldehyde (4 %), before being
453 permeabilized in PBS / 0.1% TritonX-100 for 10 min. After blocking in PBS / 0.5% BSA, cells
454 were incubated with primary antibodies overnight at 4C. Primary antibodies used are listed
455 below. Secondary Alexa Fluor Antibodies (1/600; Invitrogen) were used as described
456 previously (Kantar et al., 2021) for 1 hour at room temperature before mounting the coverslips
457 with Vectashield (Vector Laboratories #H-1200) and imaging on Zeiss Apotome or Leica
458 Thunder microscopes.
459 Antibodies used were rabbit anti-53BP1 (1/100; CST #4937), mouse anti-phospho-Histone
460 H2AX clone JBW301 (1/200; Millipore #05-636), anti-TAZ (1/100; CST #4883), mouse anti-
461 TEAD4 (1/50; Santa Cruz #sc101184), and rabbit anti-YAP (1/100; CST #14074).
462
463 ***Nuclear staining quantifications in HCT116 cells***
464 Quantification was performed using ImageJ. Binary mask corresponding to the cell nuclei was
465 based on DAPI staining. Two nuclei touching each other (and therefore recognized as one on
466 binary mask) were manually separated by drawing a 2-pixel line between them. All incomplete
467 nuclei on the edge of the image as well as those that were in mitosis or mechanically damaged
468 were excluded from the analysis. The total signal was calculated as "corrected total cell
469 fluorescence" (CTCF) according to the following formula:
470 *CTCF = Integrated Density – (Area of selected cell * Mean fluorescence of the background)*
471 Background fluorescence was measured on three different spots (roughly the size of cell
472 nucleus) outside of the cell. In case of 53BP1 and g-H2AX staining, the whole area covered by
473 the nuclear mask was quantified as one. For YAP and TAZ nuclear staining, each cell was
474 quantified separately using particle analysis tool. Cytoplasmic levels of YAP and TAZ were
475 not quantified due to the small size of the cytoplasm in HCT116 cells.
476
477 ***IC50 calculation and cytotoxicity***

478 Cell growth inhibition and cell viability after incubation with Oxaliplatin (Sigma Aldrich
479 #O9512), Verteporfin (Sigma Aldrich #SML0534), CA3 (CIL56, Selleckchem, #S8661) or
480 Dasatinib (Selleckchem #S1021) were assessed using the sulforhodamine B (SRB) assay.
481 Exponentially growing cells (750 cells/well) were seeded in 96-well plates in RPMI-1640
482 medium supplemented with 10% FCS. After 24 hours, serial dilutions of the tested drugs were
483 added and each concentration was tested in triplicate. After 96 hours, cells were fixed with
484 10% trichloroacetic acid and stained with 0.4% SRB in 1% acetic acid. SRB-fixed cells were
485 dissolved in 10 mmol/L Tris–HCl and absorbance at 540 nm was read using an MRX plate
486 reader (Dynex, Inc., Vienna, VA, USA). IC50 was determined graphically from the
487 cytotoxicity curves.
488 For HCT116-*shYAP/siTAZ*, cells were transfected in 6 well plates 24h before starting the cell
489 growth and cytotoxicity assays.
490
491 ***Quantification of the interaction effect***
492 The interaction between the drugs tested *in vitro* was investigated with a concentration matrix
493 test, in which increasing concentration of each single drug were assessed with all possible
494 combinations of the other drugs. For each combination, the percentage of expected growing
495 cells in the case of effect independence was calculated according to the Bliss equation (Greco
496 et al., 1995):
497 $$fu_c = fu_A fu_B$$
498 where fu_c is the expected fraction of cells unaffected by the drug combination in the case of
499 effect independence, and fu_A and fu_B are the fractions of cells unaffected by treatment *A* and *B,*
500 respectively. The difference between the fu_c value and the fraction of living cells in the
501 cytotoxicity test was considered as an estimation of the interaction effect, with positive values
502 indicating synergism and negative values antagonism.
503
504

505 **REFERENCES**

506 Abuetabh Y, Wu HH, Chai C, Al Yousef H, Persad S, Sergi CM, Leng R. 2022. DNA damage response
507 revisited: the p53 family and its regulators provide endless cancer therapy opportunities. *Exp Mol*
508 *Med* **54**:1658–1669. doi:10.1038/s12276-022-00863-4
509 Anders S, Huber W. 2010. Differential expression analysis for sequence count data. *Genome Biol*
510 **11**:R106. doi:10.1186/gb-2010-11-10-r106
511 Azzolin L, Panciera T, Soligo S, Enzo E, Bicciato S, Dupont S, Bresolin S, Frasson C, Basso G, Guzzardo
512 V, Fassina A, Cordenonsi M, Piccolo S. 2014. YAP/TAZ incorporation in the β-catenin destruction
513 complex orchestrates the Wnt response. *Cell* **158**:157–170. doi:10.1016/j.cell.2014.06.013
514 Azzolin L, Zanconato F, Bresolin S, Forcato M, Basso G, Bicciato S, Cordenonsi M, Piccolo S. 2012.
515 Role of TAZ as mediator of Wnt signaling. *Cell* **151**:1443–1456. doi:10.1016/j.cell.2012.11.027
516 Barry ER, Morikawa T, Butler BL, Shrestha K, de la Rosa R, Yan KS, Fuchs CS, Magness ST, Smits R,
517 Ogino S, Kuo CJ, Camargo FD. 2013. Restriction of intestinal stem cell expansion and the
518 regenerative response by YAP. *Nature* **493**:106–110. doi:10.1038/nature11693
519 Basu S, Totty NF, Irwin MS, Sudol M, Downward J. 2003. Akt phosphorylates the Yes-associated
520 protein, YAP, to induce interaction with 14-3-3 and attenuation of p73-mediated apoptosis. *Mol*
521 *Cell* **11**:11–23. doi:10.1016/s1097-2765(02)00776-1
522 Byun MR, Hwang J-H, Kim AR, Kim KM, Park JI, Oh HT, Hwang ES, Hong J-H. 2017. SRC activates TAZ
523 for intestinal tumorigenesis and regeneration. *Cancer Lett* **410**:32–40.
524 doi:10.1016/j.canlet.2017.09.003
525 Chaney S. 1995. The chemistry and biology of platinum complexes with the 1,2-diaminocyclohexane
526 carrier ligand (review). *Int J Oncol* **6**:1291–1305. doi:10.3892/ijo.6.6.1291
527 Cheung P, Xiol J, Dill MT, Yuan W-C, Panero R, Roper J, Osorio FG, Maglic D, Li Q, Gurung B, Calogero
528 RA, Yilmaz ÖH, Mao J, Camargo FD. 2020. Regenerative Reprogramming of the Intestinal Stem
529 Cell State via Hippo Signaling Suppresses Metastatic Colorectal Cancer. *Cell Stem Cell* **27**:590-
530 604.e9. doi:10.1016/j.stem.2020.07.003
531 Di Cara F, Maile TM, Parsons BD, Magico A, Basu S, Tapon N, King-Jones K. 2015. The Hippo pathway
532 promotes cell survival in response to chemical stress. *Cell Death Differ* **22**:1526–1539.
533 doi:10.1038/cdd.2015.10
534 Ege N, Dowbaj AM, Jiang M, Howell M, Hooper S, Foster C, Jenkins RP, Sahai E. 2018. Quantitative
535 Analysis Reveals that Actin and Src-Family Kinases Regulate Nuclear YAP1 and Its Export. *Cell Syst*
536 **6**:692-708.e13. doi:10.1016/j.cels.2018.05.006
537 Graham MA, Lockwood GF, Greenslade D, Brienza S, Bayssas M, Gamelin E. 2000. Clinical
538 pharmacokinetics of oxaliplatin: a critical review. *Clin Cancer Res* **6**:1205–1218.
539 Greco WR, Bravo G, Parsons JC. 1995. The search for synergy: a critical review from a response
540 surface perspective. *Pharmacol Rev* **47**:331–385.
541 Guégan J-P, Lapouge M, Voisin L, Saba-El-Leil MK, Tanguay P-L, Lévesque K, Brégeon J, Mes-Masson
542 A-M, Lamarre D, Haibe-Kains B, Trinh VQ, Soucy G, Bilodeau M, Meloche S. 2022. Signaling by the
543 tyrosine kinase Yes promotes liver cancer development. *Sci Signal* **15**:eabj4743.
544 doi:10.1126/scisignal.abj4743
545 Heng BC, Zhang X, Aubel D, Bai Y, Li X, Wei Y, Fussenegger M, Deng X. 2021. An overview of signaling
546 pathways regulating YAP/TAZ activity. *Cell Mol Life Sci* **78**:497–512. doi:10.1007/s00018-020-
547 03579-8
548 Ho KC, Zhou Z, She Y-M, Chun A, Cyr TD, Yang X. 2011. Itch E3 ubiquitin ligase regulates large tumor
549 suppressor 1 stability [corrected]. *Proc Natl Acad Sci U S A* **108**:4870–4875.
550 doi:10.1073/pnas.1101273108
551 Kantar D, Mur EB, Mancini M, Slaninova V, Salah YB, Costa L, Forest E, Lassus P, Géminard C,
552 Boissière-Michot F, Orsetti B, Theillet C, Colinge J, Benistant C, Maraver A, Heron-Milhavet L,
553 Djiane A. 2021. MAGI1 inhibits the AMOTL2/p38 stress pathway and prevents luminal breast
554 tumorigenesis. *Sci Rep* **11**:5752. doi:10.1038/s41598-021-85056-1

555 Kedan A, Verma N, Saroha A, Shreberk-Shaked M, Müller A-K, Nair NU, Lev S. 2018. PYK2 negatively
556 regulates the Hippo pathway in TNBC by stabilizing TAZ protein. *Cell Death Dis* **9**:985.
557 doi:10.1038/s41419-018-1005-z
558 Kim MH, Kim J. 2017. Role of YAP/TAZ transcriptional regulators in resistance to anti-cancer
559 therapies. *Cell Mol Life Sci* **74**:1457–1474. doi:10.1007/s00018-016-2412-x
560 Konsavage WM, Kyler SL, Rennoll SA, Jin G, Yochum GS. 2012. Wnt/β-catenin signaling regulates Yes-
561 associated protein (YAP) gene expression in colorectal carcinoma cells. *J Biol Chem* **287**:11730–
562 11739. doi:10.1074/jbc.M111.327767
563 Kopetz S, Lesslie DP, Dallas NA, Park SI, Johnson M, Parikh NU, Kim MP, Abbruzzese JL, Ellis LM,
564 Chandra J, Gallick GE. 2009. Synergistic activity of the SRC family kinase inhibitor dasatinib and
565 oxaliplatin in colon carcinoma cells is mediated by oxidative stress. *Cancer Res* **69**:3842–3849.
566 doi:10.1158/0008-5472.CAN-08-2246
567 Lamar JM, Xiao Y, Norton E, Jiang Z-G, Gerhard GM, Kooner S, Warren JSA, Hynes RO. 2019. SRC
568 tyrosine kinase activates the YAP/TAZ axis and thereby drives tumor growth and metastasis. *J Biol*
569 *Chem* **294**:2302–2317. doi:10.1074/jbc.RA118.004364
570 Lapi E, Di Agostino S, Donzelli S, Gal H, Domany E, Rechavi G, Pandolfi PP, Givol D, Strano S, Lu X,
571 Blandino G. 2008. PML, YAP, and p73 are components of a proapoptotic autoregulatory feedback
572 loop. *Mol Cell* **32**:803–814. doi:10.1016/j.molcel.2008.11.019
573 Lee K-W, Lee SS, Kim S-B, Sohn BH, Lee H-S, Jang H-J, Park Y-Y, Kopetz S, Kim SS, Oh SC, Lee J-S. 2015.
574 Significant association of oncogene YAP1 with poor prognosis and cetuximab resistance in
575 colorectal cancer patients. *Clin Cancer Res* **21**:357–364. doi:10.1158/1078-0432.CCR-14-1374
576 Levy D, Adamovich Y, Reuven N, Shaul Y. 2007. The Yes-associated protein 1 stabilizes p73 by
577 preventing Itch-mediated ubiquitination of p73. *Cell Death Differ* **14**:743–751.
578 doi:10.1038/sj.cdd.4402063
579 Li F-L, Guan K-L. 2022. The two sides of Hippo pathway in cancer. *Semin Cancer Biol* **85**:33–42.
580 doi:10.1016/j.semcancer.2021.07.006
581 Li P, Silvis MR, Honaker Y, Lien W-H, Arron ST, Vasioukhin V. 2016. αE-catenin inhibits a Src-YAP1
582 oncogenic module that couples tyrosine kinases and the effector of Hippo signaling pathway.
583 *Genes Dev* **30**:798–811. doi:10.1101/gad.274951.115
584 Li Q, Sun Y, Jarugumilli GK, Liu S, Dang K, Cotton JL, Xiol J, Chan PY, DeRan M, Ma L, Li R, Zhu LJ, Li JH,
585 Leiter AB, Ip YT, Camargo FD, Luo X, Johnson RL, Wu X, Mao J. 2020. Lats1/2 Sustain Intestinal
586 Stem Cells and Wnt Activation through TEAD-Dependent and Independent Transcription. *Cell*
587 *Stem Cell* **26**:675-692.e8. doi:10.1016/j.stem.2020.03.002
588 Lignitto L, Arcella A, Sepe M, Rinaldi L, Delle Donne R, Gallo A, Stefan E, Bachmann VA, Oliva MA,
589 Tiziana Storlazzi C, L'Abbate A, Brunetti A, Gargiulo S, Gramanzini M, Insabato L, Garbi C,
590 Gottesman ME, Feliciello A. 2013. Proteolysis of MOB1 by the ubiquitin ligase praja2 attenuates
591 Hippo signalling and supports glioblastoma growth. *Nat Commun* **4**:1822.
592 doi:10.1038/ncomms2791
593 Ling H-H, Kuo C-C, Lin B-X, Huang Y-H, Lin C-W. 2017. Elevation of YAP promotes the epithelial-
594 mesenchymal transition and tumor aggressiveness in colorectal cancer. *Exp Cell Res* **350**:218–
595 225. doi:10.1016/j.yexcr.2016.11.024
596 Liu-Chittenden Y, Huang B, Shim JS, Chen Q, Lee S-J, Anders RA, Liu JO, Pan D. 2012. Genetic and
597 pharmacological disruption of the TEAD-YAP complex suppresses the oncogenic activity of YAP.
598 *Genes Dev* **26**:1300–1305. doi:10.1101/gad.192856.112
599 Miyajima C, Kawarada Y, Inoue Y, Suzuki C, Mitamura K, Morishita D, Ohoka N, Imamura T, Hayashi
600 H. 2020. Transcriptional Coactivator TAZ Negatively Regulates Tumor Suppressor p53 Activity and
601 Cellular Senescence. *Cells* **9**:171. doi:10.3390/cells9010171
602 Morice S, Mullard M, Brion R, Dupuy M, Renault S, Tesfaye R, Brounais-Le Royer B, Ory B, Redini F,
603 Verrecchia F. 2020. The YAP/TEAD Axis as a New Therapeutic Target in Osteosarcoma: Effect of
604 Verteporfin and CA3 on Primary Tumor Growth. *Cancers (Basel)* **12**:3847.
605 doi:10.3390/cancers12123847

606 Nguyen CDK, Yi C. 2019. YAP/TAZ Signaling and Resistance to Cancer Therapy. *Trends Cancer* **5**:283–
607 296. doi:10.1016/j.trecan.2019.02.010
608 Panatta E, Zampieri C, Melino G, Amelio I. 2021. Understanding p53 tumour suppressor network.
609 *Biol Direct* **16**:14. doi:10.1186/s13062-021-00298-3
610 Perego P, Robert J. 2016. Oxaliplatin in the era of personalized medicine: from mechanistic studies to
611 clinical efficacy. *Cancer Chemother Pharmacol* **77**:5–18. doi:10.1007/s00280-015-2901-x
612 Pocaterra A, Romani P, Dupont S. 2020. YAP/TAZ functions and their regulation at a glance. *J Cell Sci*
613 **133**:jcs230425. doi:10.1242/jcs.230425
614 Raudvere U, Kolberg L, Kuzmin I, Arak T, Adler P, Peterson H, Vilo J. 2019. g:Profiler: a web server for
615 functional enrichment analysis and conversions of gene lists (2019 update). *Nucleic Acids Res*
616 **47**:W191–W198. doi:10.1093/nar/gkz369
617 Rawla P, Sunkara T, Barsouk A. 2019. Epidemiology of colorectal cancer: incidence, mortality,
618 survival, and risk factors. *Prz Gastroenterol* **14**:89–103. doi:10.5114/pg.2018.81072
619 Raymond E, Faivre S, Woynarowski JM, Chaney SG. 1998. Oxaliplatin: mechanism of action and
620 antineoplastic activity. *Semin Oncol* **25**:4–12.
621 Reggiani F, Gobbi G, Ciarrocchi A, Sancisi V. 2021. YAP and TAZ Are Not Identical Twins. *Trends*
622 *Biochem Sci* **46**:154–168. doi:10.1016/j.tibs.2020.08.012
623 Rosenbluh J, Nijhawan D, Cox AG, Li X, Neal JT, Schafer EJ, Zack TI, Wang X, Tsherniak A, Schinzel AC,
624 Shao DD, Schumacher SE, Weir BA, Vazquez F, Cowley GS, Root DE, Mesirov JP, Beroukhim R, Kuo
625 CJ, Goessling W, Hahn WC. 2012. β-Catenin-driven cancers require a YAP1 transcriptional
626 complex for survival and tumorigenesis. *Cell* **151**:1457–1473. doi:10.1016/j.cell.2012.11.026
627 Salah Z, Melino G, Aqeilan RI. 2011. Negative regulation of the Hippo pathway by E3 ubiquitin ligase
628 ITCH is sufficient to promote tumorigenicity. *Cancer Res* **71**:2010–2020. doi:10.1158/0008-
629 5472.CAN-10-3516
630 Shao DD, Xue W, Krall EB, Bhutkar A, Piccioni F, Wang X, Schinzel AC, Sood S, Rosenbluh J, Kim JW,
631 Zwang Y, Roberts TM, Root DE, Jacks T, Hahn WC. 2014. KRAS and YAP1 converge to regulate
632 EMT and tumor survival. *Cell* **158**:171–184. doi:10.1016/j.cell.2014.06.004
633 Sirvent A, Mevizou R, Naim D, Lafitte M, Roche S. 2020. Src Family Tyrosine Kinases in Intestinal
634 Homeostasis, Regeneration and Tumorigenesis. *Cancers (Basel)* **12**:E2014.
635 doi:10.3390/cancers12082014
636 Song S, Xie M, Scott AW, Jin J, Ma L, Dong X, Skinner HD, Johnson RL, Ding S, Ajani JA. 2018. A Novel
637 YAP1 Inhibitor Targets CSC-Enriched Radiation-Resistant Cells and Exerts Strong Antitumor
638 Activity in Esophageal Adenocarcinoma. *Mol Cancer Ther* **17**:443–454. doi:10.1158/1535-
639 7163.MCT-17-0560
640 Steinhardt AA, Gayyed MF, Klein AP, Dong J, Maitra A, Pan D, Montgomery EA, Anders RA. 2008.
641 Expression of Yes-associated protein in common solid tumors. *Hum Pathol* **39**:1582–1589.
642 doi:10.1016/j.humpath.2008.04.012
643 Strano S, Monti O, Pediconi N, Baccarini A, Fontemaggi G, Lapi E, Mantovani F, Damalas A, Citro G,
644 Sacchi A, Del Sal G, Levrero M, Blandino G. 2005. The transcriptional coactivator Yes-associated
645 protein drives p73 gene-target specificity in response to DNA Damage. *Mol Cell* **18**:447–459.
646 doi:10.1016/j.molcel.2005.04.008
647 Strano S, Munarriz E, Rossi M, Castagnoli L, Shaul Y, Sacchi A, Oren M, Sudol M, Cesareni G, Blandino
648 G. 2001. Physical interaction with Yes-associated protein enhances p73 transcriptional activity. *J*
649 *Biol Chem* **276**:15164–15173. doi:10.1074/jbc.M010484200
650 Tapon N, Harvey KF, Bell DW, Wahrer DCR, Schiripo TA, Haber DA, Hariharan IK. 2002. salvador
651 Promotes both cell cycle exit and apoptosis in Drosophila and is mutated in human cancer cell
652 lines. *Cell* **110**:467–478. doi:10.1016/s0092-8674(02)00824-3
653 Tesniere A, Schlemmer F, Boige V, Kepp O, Martins I, Ghiringhelli F, Aymeric L, Michaud M, Apetoh L,
654 Barault L, Mendiboure J, Pignon J-P, Jooste V, van Endert P, Ducreux M, Zitvogel L, Piard F,
655 Kroemer G. 2010. Immunogenic death of colon cancer cells treated with oxaliplatin. *Oncogene*
656 **29**:482–491. doi:10.1038/onc.2009.356

657 Thompson BJ. 2020. YAP/TAZ: Drivers of Tumor Growth, Metastasis, and Resistance to Therapy.
658 *Bioessays* **42**:e1900162. doi:10.1002/bies.201900162
659 Totaro A, Panciera T, Piccolo S. 2018. YAP/TAZ upstream signals and downstream responses. *Nat Cell*
660 *Biol* **20**:888–899. doi:10.1038/s41556-018-0142-z
661 Touil Y, Igoudjil W, Corvaisier M, Dessein A-F, Vandomme J, Monté D, Stechly L, Skrypek N, Langlois
662 C, Grard G, Millet G, Leteurtre E, Dumont P, Truant S, Pruvot F-R, Hebbar M, Fan F, Ellis LM,
663 Formstecher P, Van Seuningen I, Gespach C, Polakowska R, Huet G. 2014. Colon cancer cells
664 escape 5FU chemotherapy-induced cell death by entering stemness and quiescence associated
665 with the c-Yes/YAP axis. *Clin Cancer Res* **20**:837–846. doi:10.1158/1078-0432.CCR-13-1854
666 Vasan N, Baselga J, Hyman DM. 2019. A view on drug resistance in cancer. *Nature* **575**:299–309.
667 doi:10.1038/s41586-019-1730-1
668 Wang C, Zhu X, Feng W, Yu Y, Jeong K, Guo W, Lu Y, Mills GB. 2016. Verteporfin inhibits YAP function
669 through up-regulating 14-3-3σ sequestering YAP in the cytoplasm. *Am J Cancer Res* **6**:27–37.
670 Woynarowski JM, Chapman WG, Napier C, Herzig MC, Juniewicz P. 1998. Sequence- and region-
671 specificity of oxaliplatin adducts in naked and cellular DNA. *Mol Pharmacol* **54**:770–777.
672 doi:10.1124/mol.54.5.770
673 Woynarowski JM, Faivre S, Herzig MC, Arnett B, Chapman WG, Trevino AV, Raymond E, Chaney SG,
674 Vaisman A, Varchenko M, Juniewicz PE. 2000. Oxaliplatin-induced damage of cellular DNA. *Mol*
675 *Pharmacol* **58**:920–927. doi:10.1124/mol.58.5.920
676 Xie Y-H, Chen Y-X, Fang J-Y. 2020. Comprehensive review of targeted therapy for colorectal cancer.
677 *Signal Transduct Target Ther* **5**:22. doi:10.1038/s41392-020-0116-z
678 Yoshikawa K, Noguchi K, Nakano Y, Yamamura M, Takaoka K, Hashimoto-Tamaoki T, Kishimoto H.
679 2015. The Hippo pathway transcriptional co-activator, YAP, confers resistance to cisplatin in
680 human oral squamous cell carcinoma. *Int J Oncol* **46**:2364–2370. doi:10.3892/ijo.2015.2948
681 Zeng R, Dong J. 2021. The Hippo Signaling Pathway in Drug Resistance in Cancer. *Cancers (Basel)*
682 **13**:318. doi:10.3390/cancers13020318
683 Zheng Y, Pan D. 2019. The Hippo Signaling Pathway in Development and Disease. *Dev Cell* **50**:264–
684 282. doi:10.1016/j.devcel.2019.06.003
685

686

687

ACKNOWLEDGEMENTS

The authors thank the different lab members of the Djiane and Gongora teams for helpful discussions. VS was supported by Fondation de France. MR was supported by LabEx NUMEV. DK was supported by Ligue Contre le Cancer. This work was supported by grants from Fondation ARC (#PJA 20141201630) and Ligue Nationale Contre le Cancer (Région Languedoc-Roussillon) to LHM and AD. Work in the lab of CG was also supported by grants and funds from INSERM, the Institut du cancer de Montpellier (ICM), SIRIC (SIRIC Montpellier Cancer Grant «INCa-DGOS-Inserm 6045»), Cancéropole GSO, and the program «investissement d'avenir» (grant agreement: Labex MabImprove, ANR-10-LABX-53-01).

AUTHOR CONTRIBUTIONS

VS, LHM, LJ, and DK performed experiments. CG and AD designed the experiments. VS, LHM, MR, DK, CG and AD analyzed the data. VS, LHM, DT, LB, CG, and AD interpreted the data. CG and AD wrote the manuscript.

COMPETING INTERESTS

All authors declare no competing interest

708 **FIGURE LEGENDS**

709 **Figure 1. Oxaliplatin treatment induces DNA damage**

710 **A**. Immunofluorescence experiments performed on HCT116 cells treated, or not, with
711 oxaliplatin (0.5 μM) monitoring γ-H2AX (yellow). DAPI (blue) was used to stain DNA and
712 the nuclei. Quantification of the staining is shown on the right side and is represented as the
713 corrected nuclear fluorescence. Data are represented as the mean ± SEM. (n=3). Unpaired two-
714 tailed Student's t-test; ** $p<0.01$.

715 **B**. Immunofluorescence experiments performed on HCT116 cells treated, or not, with
716 oxaliplatin (0.5 μM) monitoring 53BP1 (grey). DAPI (blue) was used to stain DNA and the
717 nuclei. Quantification of the staining is shown on the right side and is represented as the
718 corrected nuclear fluorescence. Data are represented as the mean ± SEM. (n=3). Unpaired two-
719 tailed Student's t-test; *** $p<0.001$.

720 **C**. Western blot analysis showing protein expression of TEAD4 and p53 family of proteins in
721 HCT116 treated (Oxa), or not (NT) with oxaliplatin (0.5 μM). GAPDH was used as a loading
722 control (n=3).

723 **D.** Heat map corresponding to the genes differentially expressed in HCT116 cells after 24h of
724 oxaliplatin treatment at IC50 (see Supplemental Table 1). The three replicates for the non-
725 treated (NT) and treated (Oxa) are shown.

726

727 **Figure 2. Oxaliplatin treatment triggers YAP and TAZ nuclear accumulation**

728 **A**. Immunofluorescence experiments performed on HCT116 cells treated, or not, with
729 oxaliplatin (0.5 μM) monitoring TEAD4 (top panels), YAP (middle panels), and TAZ (bottom
730 panels) nuclear localization (red). DAPI (blue) was used to stain DNA and the nuclei.
731 Quantification of both stainings are shown on the right side of the figures and are represented
732 as the corrected nuclear fluorescence. Data are represented as the mean ± SEM (n=3). Unpaired
733 two-tailed Student's t-test; **** $p < 0.0001$.

734 **B**. Western blot analysis showing protein expression and/or activation of Hippo pathway
735 components in HCT116 cells treated (Oxa), or not (NT) with oxaliplatin (0.5 μM). GAPDH
736 was used as a loading control (n=3).

737 **C**. Western blot analysis after subcellular fractionation showing the relative amount of YAP
738 and TAZ protein in the nuclear fraction of HCT116 cells treated (Oxa), or not (NT) with
739 oxaliplatin (0.5 μM). Histone H3 was used as a nuclear loading control for the fractionation
740 (n=3).

741

742 **Figure 3. YAP and TAZ are required for oxaliplatin-mediated cell death**

743 **A**. HCT116-*shYAP* and HCT116-*shLuc* cell lines were treated with increasing doses of
744 oxaliplatin for 96h. Cell viability analysis was then assessed using SRB assay and the IC50 of
745 oxaliplatin was calculated as the concentration needed to kill 50% of the cells (shown in the
746 inset). Paired two-tailed Student's t-test ,* $p<0.05$.

747 **B**. HCT116-*shYAP-siTAZ* and HCT116-*shLuc-siCtl* (control) cell lines were treated with
748 increasing doses of oxaliplatin for 96h. Cell viability analysis was then assessed using SRB
749 assay and the IC50 of oxaliplatin was calculated as the concentration needed to kill 50% of the
750 cells (shown in the inset). Paired two-tailed Student's t-test, ** $p<0.01$.

751 **C**. Western blot analysis showing protein expression of TAZ and YAP in HCT116-*shLuc*, -
752 *siTAZ*, -*shYAP* and both -*shYAP-siTAZ* used in panel A and B. Tubulin was used as a loading
753 control (n=3).

754 **D**. HCT116 cells were incubated with increasing concentrations of oxaliplatin and either
755 Verteporfin or CA3. Cell viability was assessed with the SRB assay in 2D to obtain the viability
756 matrix. Drug concentrations were as follows: Verteporfin (from 0.437 to 7 µM), CA3 (from
757 0.004 to 0.75 µM) and oxaliplatin (from 0.0185 to 1.2 µM). The synergy matrices were
758 calculated as described in Materials and Methods.

759

760 **Figure 4. Src inhibition by Dasatinib reduces HCT116 cells sensitivity to oxaliplatin**

761 **A**. Western blot analysis showing protein expression of YAP and TAZ in HCT116 treated, or
762 not, with oxaliplatin (0.5 µM) and/or Dasatinib (50 nM and 100 nM). Phopsho-SRC blotting
763 was used to evaluate the inhibition of SRC activity using Dasatinib. GAPDH was used as a
764 loading control (n=3). Quantification of the blots (performed using Image J software) is shown
765 on the right side of the figure.

766 **B**. Immunofluorescence experiments performed in HCT116 cells treated, or not, with
767 oxaliplatin (0.5 µM) and/or Dasatinib (50 nM) monitoring YAP (top panels) and TAZ (bottom
768 panels) nuclear localization (red). DAPI (blue) was used to stain DNA and the nuclei.
769 Quantification of both stainings are shown on the right side of the figures and are represented
770 as the corrected nuclear fluorescence. Data are represented as the mean ± SEM (n=3). Unpaired
771 two-tailed Student's t-test; ****$p < 0.0001$.

772 **C**. HCT116 colorectal cancer cell lines were incubated with increasing concentrations of
773 oxaliplatin and Dasatinib. Cell viability was assessed with the SRB assay in 2D to obtain the
774 viability matrix. Drug concentrations were as follows: Dasatinib (from 1 to 16 µM) and

775 oxaliplatin (from 0.0185 to 1.2 μM). The synergy matrix was calculated as described in
776 Materials and Methods.
777
778
779
780 **SUPPLEMENTAL FIGURE LEGENDS**
781
782 **Supplemental Figure 1. Cell viability in response to drugs**
783 Cells were treated with increasing doses of oxaliplatin (**A**), Verteporfin (**B**), CA3 (**C**) and
784 Dasatinib (**D**) for 96h. Cell viability analysis was then assessed using SRB assay and the IC50
785 of each drug could be calculated as the concentration that reduced cell numbers by 50% (shown
786 in the insets).
787
788 **Supplemental Figure 2. Interaction between YAP/TAZ and P53 protein family members**
789 **in HCT116 cells**
790 Western blot analysis of Flag (YAP or TAZ) immunoprecipitates on protein extracts from
791 HCT116 treated (Oxa), or not (NT) showing an interaction between YAP and p73 (n=3).
792
793 **Supplemental Table 1. Differentially expressed genes in HCT116 cells after oxaliplatin**
794 **treatment for 24h at IC50**
795 Only differentially expressed genes with an adjusted p-value< 0.05 are shown. Columns are:
796 test_id: position and description of the feature tested
797 ENSG_ID: Ensemble gene ID
798 symbol: gene symbol
799 sample_1: first group in the comparison; untreated cells
800 sample_2: second group in the comparison; cells treated with oxaliplatin
801 mean_1: mean of normalized count for the first group in the comparison
802 mean_2: mean of normalized count for the second group in the comparison
803 log2FoldChange: log2 fold change estimates
804 pvalue: pvalue
805 padj: pvalue adjusted for multiple testing with the Benjamini-Hochberg procedure, which
806 controls false discovery rate (FDR)
807
808

Supplemental Table 2. g:profiler functional enrichment analyses

Columns are :

GO_ID: Gene Ontology

KEGG_ID: KEGG pathways

REAC_ID: Reactome pathways

WP_ID: WikiPathways

TF_ID: regulatory motif matches from TRANSFAC

MIRNA_ID: miRNA targets from miRTarBase

CORUM_ID: protein complexes from CORUM

HPA_ID: tissue specificity from Human Protein Atlas

HP_ID: human disease phenotypes from Human Phenotype Ontology

Description: description of the functional group

p.Val: p-value

FDR: false discovery rate

Genes: genes found in the intersection

Slaninova et al. Figure 1

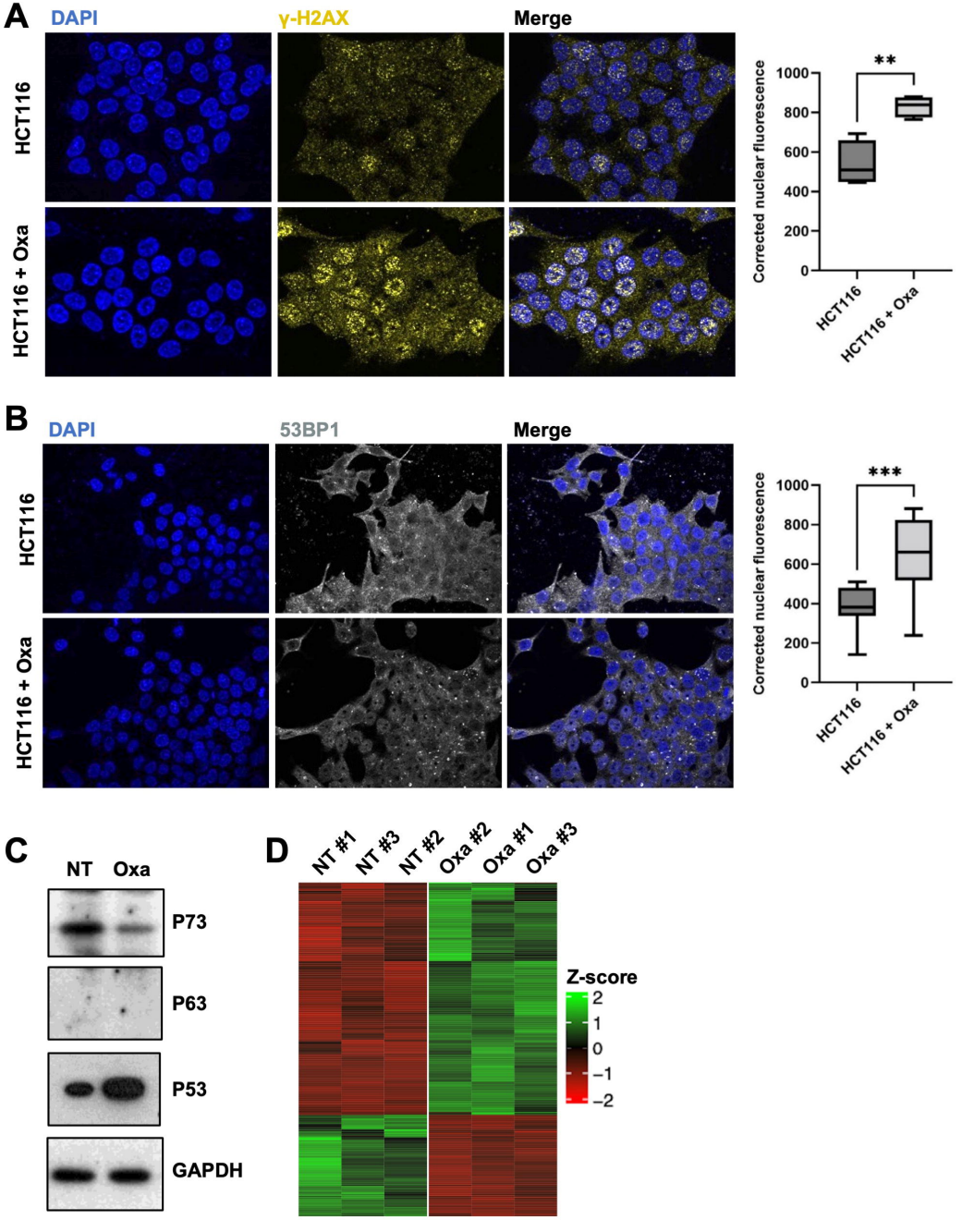

Slaninova et al. Figure 2

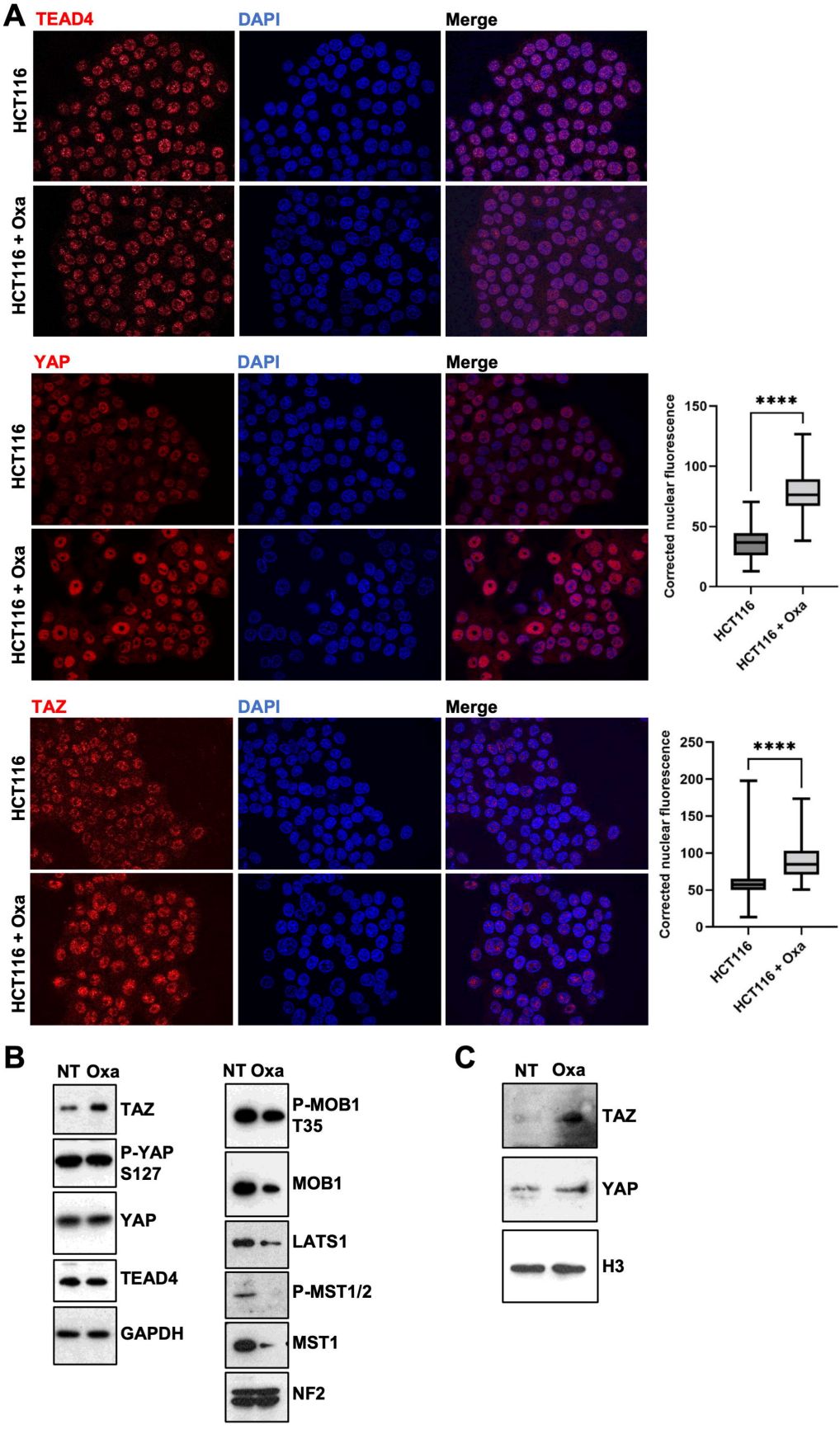

Slaninova et al. Figure 3

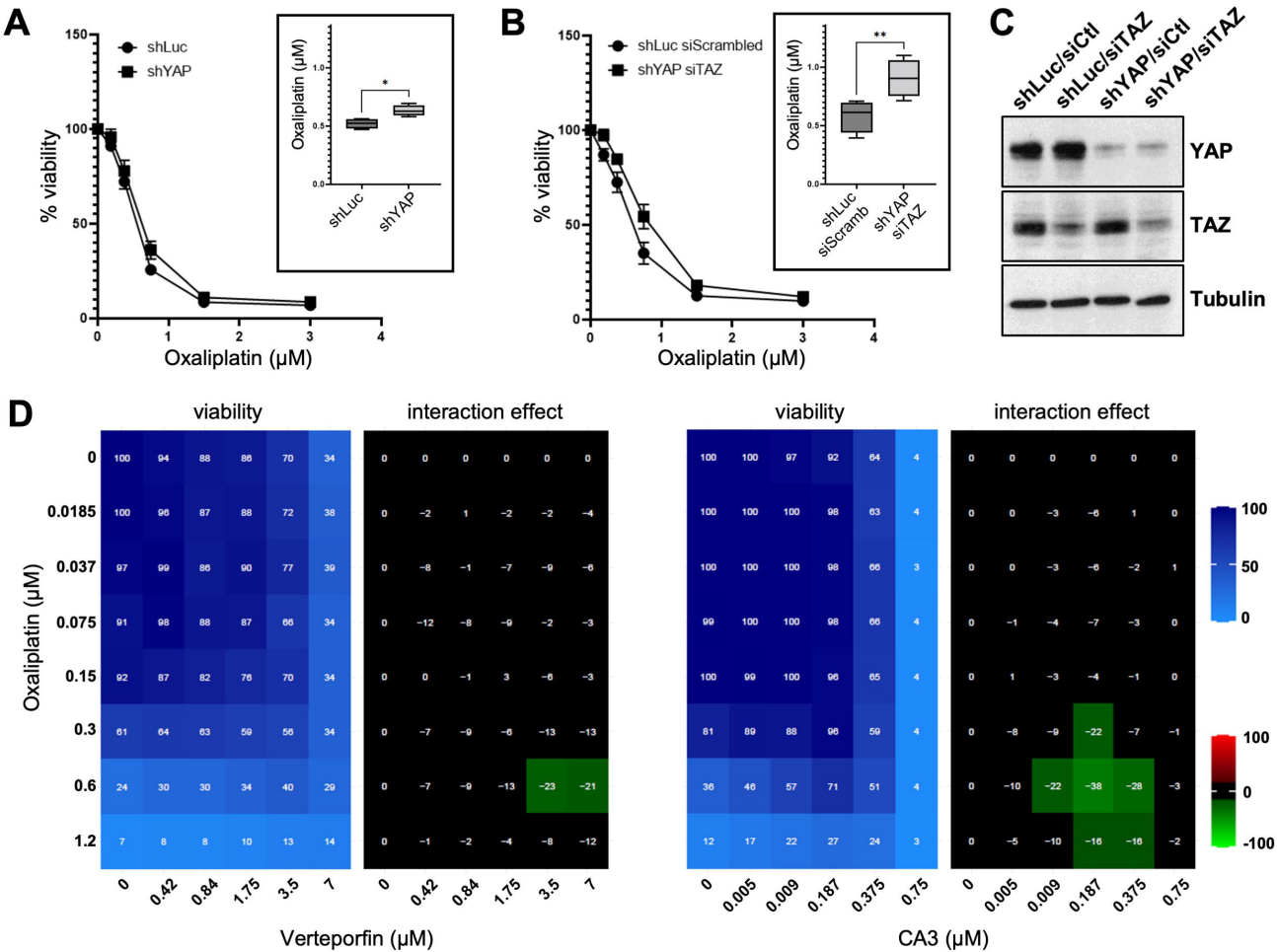

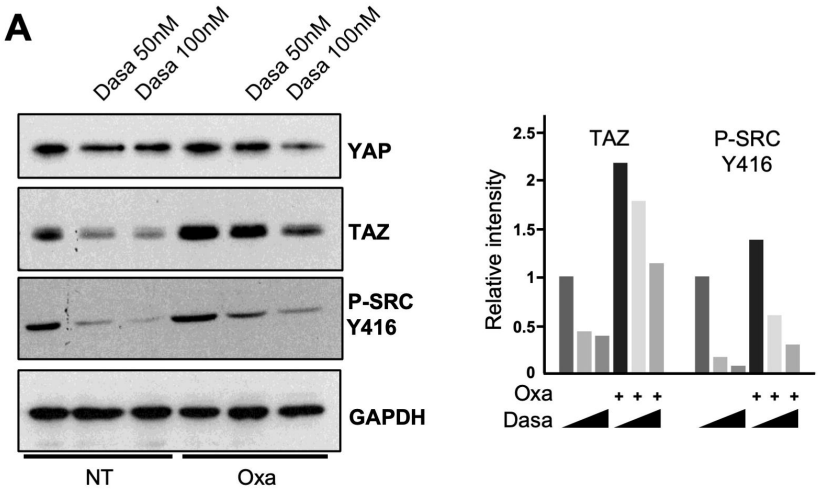
A
Dasa 50nM
Dasa 100nM
Dasa 50nM
Dasa 100nM
YAP
TAZ
P-SRC Y416
GAPDH
NT
Oxa
TAZ
P-SRC Y416
Relative intensity
2.5
2
1.5
1
0.5
0
Oxa
Dasa
+ + +
+ + +

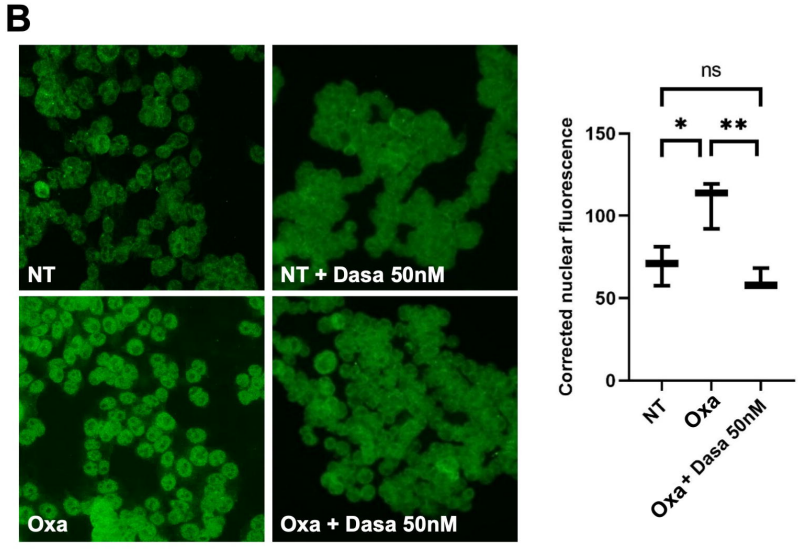
B
NT
NT + Dasa 50nM
Oxa
Oxa + Dasa 50nM
ns
*
**
Corrected nuclear fluorescence
150
100
50
0
NT
Oxa
Oxa + Dasa 50nM

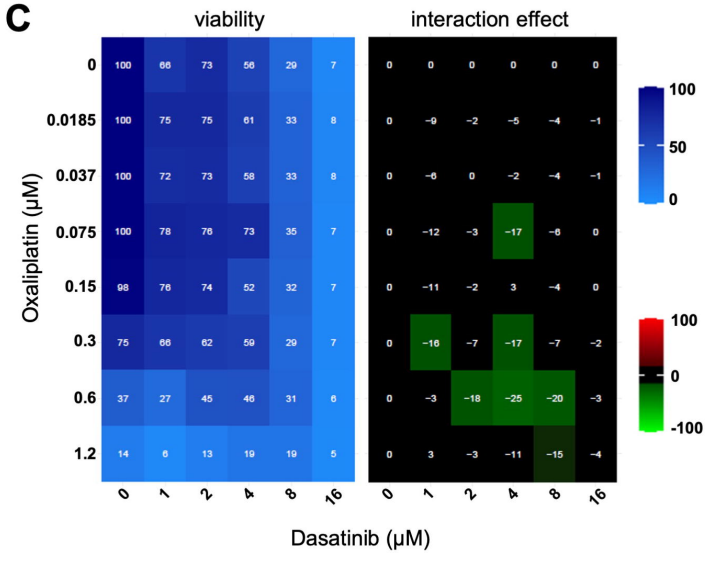
C
viability
interaction effect
Oxaliplatin (μM)
0
0.0185
0.037
0.075
0.15
0.3
0.6
1.2
0 1 2 4 8 16
Dasatinib (μM)
100
50
0
100
0
-100